The Journal of Experimental Biology 207, 3003-3014
Published by The Company of Biologists 2004
doi:10.1242/jeb.01116

The effects of intense wing molt on diving in alcids and potential influences on the evolution of molt patterns

Eli S. Bridge

University of Minnesota Department of Ecology, Evolution, and Behavior, 100 Ecology Building, 1987 Upper Buford Circle, Saint Paul, MN 55108, USA

Address for correspondence: University of Memphis Biology Department, 5700 Walker Avenue, 103 Ellington Hall, Memphis, TN 38152-3540, USA (e-mail: ebridge@memphis.edu)

Accepted 26 May 2004

Summary

Large and medium-sized alcids have a very intense wing molt wherein many flight feathers are shed in rapid succession and wing surface area is reduced by as much as 40%. Although these birds are rendered flightless during wing molt, they must still use their wings to propel themselves underwater. A molt-induced loss of wing area could simply reduce wing propulsion such that more muscular work would be required to maintain a given speed. Alternatively, molt could reduce drag on the wings, making a bird more penguin-like and actually enhancing diving ability. I addressed this issue by filming captive common guillemots *Uria aalge* and tufted puffins *Fratercula cirrhata* using an array of video cameras to plot the birds' movements in three dimensions. From these coordinate data I calculated swimming velocities, angles of descent and absolute depths. These values allowed me to estimate the forces due to drag and buoyancy that must be counteracted by flapping, which in turn yielded estimates of the amount of work generated during each flap as well as the average power and cost of transport. Within-bird comparisons of diving performance when wings were intact and during several stages of wing molt indicated that molt is associated with more frequent flapping, reduced displacement during the flap cycle, and possibly reduced work per flap. These negative effects on diving may explain why primary and secondary molts were offset in the birds I studied such that the period during which all of the flight feathers are effectively missing is minimized.

Movies available on-line

Key words: molt, wing-propelled diving, *Uria aalge*, *Fratercula cirrhata*, biomechanics, video analysis, mechanical efficiency, flap cycle.

Effects of moult on diving

For most birds the replacement of flight feathers is the most challenging component of the molting process as it requires a high energetic and nutritional investment to grow what are typically a bird's largest feathers (Walsberg, 1983; Murphy and King, 1991; Murphy, 1996; Klasing, 1998) and because the temporary loss of flight feathers may compromise wing-propelled locomotion (Tucker, 1991; Hedenström and Sunada, 1999; Bridge, 2003; Williams and Swaddle, 2003). Most studies of the effects of wing molt on locomotion have been restricted to aerial flight performance. Yet in a number of birds including alcids (Alcidae), diving petrels (Pelecanoididae), dippers (Cinclidae) and some shearwaters (*Puffinus* spp.), the wings are used to power underwater diving as well as aerial flight, and molt of the flight feathers is likely to influence diving biomechanics in these species.

Medium-sized and large alcids (Alcidae) undergo a relatively intense wing molt, wherein the flight feathers are shed in short succession (usually within 2 weeks). In most alcids this molt takes place in the fall, shortly after the breeding season (Ewins, 1993; Gaston and Jones, 1998; Thompson et al., 1998; Thompson and Kitaysky, 2004), and causes a substantial loss of wing surface area rendering a molting bird temporarily flightless. Yet these birds must continue to dive underwater throughout wing molt to forage and perhaps to avoid predators. This situation begs the question of how a molt-induced loss of wing area affects the capacity for the wings to propel an alcid underwater. However, prior to this study there has been only one examination of the effect of wing molt on diving, and dive speed was the only parameter measured (Swennen and Duiven, 1991).

Studies of the effects of wing molt on aerial flight generally indicate that molt reduces flight ability and/or efficiency (Tucker, 1991; Swaddle and Witter, 1997; Hedenström and Sunada, 1998; Chai et al., 1999; Swaddle et al., 1999; Bridge, 2003), and we might expect the same to be true for underwater diving. However, some have speculated that the opposite may be true for the effects of flight-feather molt on wing-propelled diving (Thompson et al., 1998; Keitt et al., 2000; Montevecchi

and Stenhouse, 2002). Birds that use their wings underwater must balance morphological trade-offs between evolutionary pressures associated with aerial flight and underwater diving (Storer, 1960; Stresemann and Stresemann, 1966; Ashmole, 1971; Pennycuick, 1987; Raikow et al., 1988; Kovacs and Meyers, 2000). A presumed indication of such a trade-off is the fact that many diving birds have small wings relative to body size (i.e. high wing loading). Although these small wings allow for little maneuverability and require high speeds and flap rates for aerial flight, they may be more effective than large wings for underwater propulsion as large wings would create inordinate drag (Thompson et al., 1998; Keitt et al., 2000; Montevecchi and Stenhouse, 2002). Following this line of reasoning, a molt-induced loss of wing area could cause an increase in diving ability and/or efficiency.

The goal of this study was to use a video triangulation technique to closely monitor the underwater movements of captive alcids in such a way that I could measure parameters such as flap duration, speed, work per flap, cost of transport, and power throughout a period of wing molt. Because the effects of molt on these diving parameters are difficult to predict, I tested the null hypothesis that molt would have no effect on any of these diving parameters.

Materials and methods

Study site

All filming took place at SeaWorld California (500 Seaworld Drive, San Diego, CA, USA), where approximately 40 common guillemots *Uria aalge* Pontoppidau, 50 tufted puffins *Fratercula cirrhata* Pallas and five rhinoceros auklets *Cerorhinca monocerata* are housed communally as part of an exhibit called ‘The Penguin Encounter’. The alcids live in a naturalistic habitat complete with a large (ca. 72 000 l) pool that allows for underwater diving. The aviary is bounded on one side by a viewing window approximately 21 m long and 2.5 m tall, which allows observation of the birds both above and below the water’s surface. The depth of the pool varies considerably, with a maximum of approximately 3 m. Lighting in the habitat came primarily from an array of skylights such that the birds experienced normal daylength cycles for southern California during the winter. There was additional artificial lighting, which is used to lengthen daylight periods during the summer to simulate the light cycle at 60°N latitude.

During the period of data collection for this study, the birds were fed a fish diet consisting of several species (e.g. Atlantic silversides *Menidia menidia* and herring, *Clupea* spp.). Food was available *ad libitum* in trays located throughout the aviary, and husbandry staff threw thawed fish into the diving pool at four regular feedings every day. Diving activity generally peaked during these feeding times, but there was usually sporadic diving throughout the day.

Camera array and filming

I used an array of four small black-and-white CCD video cameras (model YK-3027D, Iou Ken Electronic Co., Taipei, Taiwan) to film diving activity within a small portion of the pool. The cameras were arranged as two pairs, which viewed the same section of the pool from two different angles. One camera of each pair was mounted in front of the viewing window (referred to henceforth as a frontal camera), and the other was mounted above the pool pointing straight down (referred to as an overhead camera). Thus, a bird diving within the observational field of the cameras would be filmed from above and from the side simultaneously.

Signals from the cameras were routed through a video processor (model YK-9003, Iou Ken Electronic Co., Taipei, Taiwan), which combined the inputs from the four video cameras into a composite image with the views of each video camera occupying a fourth of the video screen. This composite footage was then digitally recorded on a Sony Digtial8 Camcorder at 30 frames s^{-1}. An example of a video-taped dive is available at http://jeb.biologist.org.

Generation of three-dimensional position data

In order to calibrate the measurement system to obtain measurements in SI units from the video footage, I fashioned a T-shaped apparatus made of white 2.5 cm (diameter) polyvinyl chloride (PVC) tubing (henceforth called the T-pipe), and with assistance from the SeaWorld staff, had it placed in strategic positions within the diving pool. The T-pipe measured 1.12 m across the top and had several detachable sections incorporated into the stem that allowed the video cameras to record known lengths marked on the T-pipe at known distances from the inside surface of the viewing window or from the surface of the water. For the frontal cameras, this calibration procedure involved placing the stem of the T-pipe against the glass and extending it horizontally directly away from each camera, such that the top of the T-pipe was distanced from the glass surface by an amount equal to the length of the stem. By adding 0.45 m and 0.70 m sections of tubing to the stem in any combination, the distance between the span of tubing at the top of the T-pipe and the video camera could be altered by known intervals. I used similar procedures to calibrate the overhead cameras, but in this case the T-pipe was held vertically and upside-down directly beneath the cameras.

To generate measures of the speed and depth of each dive from the digital video footage, I first had to plot the birds’ positions from each camera onto a two-dimensional coordinate system. After trimming the dive footage to remove unwanted parts of a dive (i.e. turning, stopping, gliding and the first few flaps of a dive), I converted the image into QuickTime JPEG format with a screen size of 1000×750 pixels. I used the program CamMotion v0.9.5 (TERC, Cambridge, MA, http://projects.terc.edu/cam/cam_homepage.html) to map the position of a bird throughout a dive from both overhead and frontal views onto a Cartesian coordinate system that used pixels as units.

The coordinate data from both the overhead and frontal cameras went through several transformations in order to yield three-dimensional coordinates in SI units. Firstly, the video

cameras I used generated a somewhat distorted image in which a flat surface would have a convex appearance. This phenomenon is known as barrel distortion (so named because a rectangle would be made to appear barrel-shaped) and is a common shortcoming of inexpensive camera lenses. I corrected for this barrel distortion by converting the Cartesian coordinates to radial coordinates and applying a second-order polynomial function that increased each point's radial distance as a function of the initial radial distance (r):

Scaled radial distance =

$$r/(-0.00000r^2 + 0.00006474r + 1)\,. \quad (1)$$

The values used in this equation are particular to the cameras employed in this study and were derived by a calibration process wherein I filmed a flat wall with an array of dots spaced at known intervals that allowed me to calculate the extent to which the image was distorted as a function of the radial distance from the center of the field of view.

A second correction was needed to ensure that the angles of each dive were calculated with respect to true horizontal. I used the surface of the water as viewed from the frontal cameras as a standard for true horizontal and rotated the radial coordinates from the frontal cameras according to the slope of the water's surface in the video. I performed a similar correction on data from the overhead cameras except that the correction was made with reference to the surface of the viewing window (i.e. perpendicular to the associated frontal camera).

After conversion of the transformed and rotated radial coordinates back to x–y coordinates, the data were scaled such that the surface of the water was set to y=0 and that all y coordinates for a diving bird were negative numbers. These new Cartesian coordinates were then converted from pixels to meters using scale factors generated from the calibration footage.

Triangulation of a bird's position in the pool was complicated by the fact that light from within the water was refracted as it moved through the water–air interface or the water–glass–air interface before reaching a camera. I dealt with this problem by using the calibration footage to estimate the apparent position of the camera relative to the water. This apparent position is where the camera appeared to be according to how the length of a piece of plastic pipe changed on the video screen as its proximity to the camera was increased by known intervals. I used the following equation to model the visual length of the pipe (L) as a function of its distance (D) from the water's surface or the water–window interface:

$$L = L_0 \times D_C / (D+D_C)\,, \quad (2)$$

where the constants L_0 and D_C are the length of the pipe at D=0 and the apparent distance of the camera from the water, respectively. Thus, as the pipe's distance from the camera doubles such that D=D_C, its length on the screen is reduced by half. After fitting the data from calibration footage (leveled and corrected for barrel distortion as described above) to Equation 2, I estimated the apparent distance of each camera from the water by extrapolating the value of D for which L was halved and using this value of D to derive D_C.

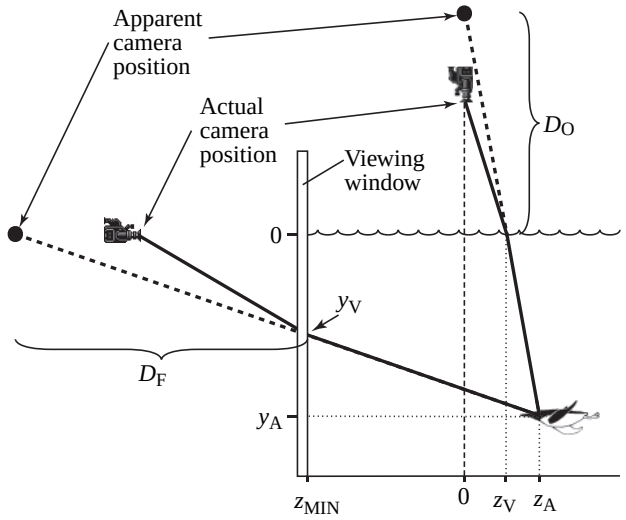

Fig. 1. Illustration of the video triangulation technique used to generate three-dimensional coordinate data. The y axis for the coordinate system is the vertical broken line associated with the 0 value for z. The z axis is the water surface, such that all underwater coordinates have negative y values. See text for explanations of all variables.

Once the apparent distance of the camera was known, the two-dimensional surface maps of bird positions from the overhead and frontal points of view were then combined to triangulate the true positions of a bird in three-dimensional space. I defined coordinates according to three axes: x, the horizontal axis parallel to the viewing window; y, the vertical axis (depth); and z, the horizontal axis perpendicular to the viewing window. Fig. 1 illustrates how the actual z and y coordinates (z_A and y_A) can be found, given z and y coordinates as they appear in the video footage (z_V and y_V) and the apparent positions of the overhead and frontal cameras relative to the surface of the water and the water–window interface, respectively. The perpendicular distances between the water and the camera are defined as D_O with respect to the overhead camera and D_F with respect to the frontal camera. The surface of the water defined the zero value for y, such that all y values for diving birds were negative. The zero value of the z axis was defined by the position of the overhead camera such that the z equaled 0 directly below the camera and z increased with the distance from the water-window interface. The water–window interface defined the lowest possible z value, z_{MIN}. To derive z_A and y_A, I used the coordinates of the apparent camera positions along with z_V and y_V to establish equations for lines that link the actual position of the bird with each of the apparent camera positions, which are shown below in slope–intercept form with z_A as the independent variable:

For the frontal camera:

$$y_A = z_A\left(\frac{y_V}{D_F}\right) + y_V\left(1 - \frac{z_{MIN}}{D_F}\right). \quad (3)$$

and for the overhead camera:

$$y_A = z_A\left(\frac{-D_O}{z_Y}\right) + D_O\,. \quad (4)$$

These equations can then be used to solve for z_A as follows:

$$z_A = \frac{D_O - y_V\left(1 - \frac{z_{MIN}}{D_F}\right)}{\left(\frac{y_V}{D_F}\right) + \left(\frac{D_O}{z_V}\right)}\,. \quad (5)$$

One can then find y_A using either Equation 3 or 4. I used a similar series of calculations to determine the actual value for x. Because the paired sets of cameras overlapped in their fields of view to a small extent, I was able to consolidate position data from birds that swam through both fields of view by simply appending the relative position data from the second half of a dive to that of the first half.

Before using this system of video triangulation to measure dive parameters I tested the system with the calibration footage by finding the three-dimensional positions of the opposite ends of a 0.56 m piece of PVC tubing in a variety of locations throughout the monitored area of the diving pool. After establishing the accuracy of the measurement system (see Results), I generated coordinate data for diving birds using CamMotion to record the initial coordinates and an Excel spreadsheet to perform the necessary transformations and triangulation of the data.

Derivation of dive parameters

As with other attempts to measure biomechanical properties of wing-propelled diving (Lovvorn et al., 1999; Lovvorn, 2001; Lovvorn and Liggins, 2002), I employed a model that conceives a bird's body and wings as a fuselage and a propulsion system, respectively. The propulsion system can then be evaluated by observing its capacity to counter the forces that resist forward movement of the fuselage. This approach avoids the need to invoke complex models of fluid vorticity around the wings, which would have to take into account varying wing shape, surface area and rotational velocity (Dickinson, 1996). My approach was further simplified by using the flap cycle as the measurement interval of interest. As average speed remained relatively constant from one flap cycle to the next, I ignored inertial work (work associated with changes in velocity) in my calculations as this parameter would sum to zero over a flap, with negative work from deceleration during passive phases of the flap cycle counteracting positive work from acceleration during active stroke phases.

Although I present several measures of diving efficiency in this paper, including measures of work and power, they are all generated from three basic measurements: displacement, dive angle (relative to horizontal), and absolute depth. For example, estimates of drag were calculated based on rates of displacement or speed. These estimates were generated using equations specific to common guillemots and tufted puffins derived from empirical tests of drag *versus* speed performed on frozen specimens in a tow tank (Lovvorn et al., 2001; Lovvorn and Liggins, 2002).

The measurements of dive angle and absolute depth were necessary to calculate the degree to which buoyancy was opposing the forward motion of the bird. Buoyancy in diving birds decreases with depth in direct proportion to the reduction of air volumes in the plumage and lungs. I estimated these air volumes using published data from common guillemots and other diving birds. Estimates of plumage air volume came from a measurement of 0.33 l kg^{-1} obtained by Wilson et al. (1992), who compared water displacement of dead common guillemots before and after flooding the plumage. In estimating this residual respiratory air volume I followed the procedures of Wilson et al. (1992), who employed an allometric equation from Lasiewski and Calder (1971) to derive an estimate of 0.173 l for a common guillemot weighing 1.087 kg (i.e. 0.160 l kg^{-1}).

The contribution of the body tissues to buoyancy was calculated from body composition following the same procedures (Lovvorn et al., 1999) used to estimate buoyancy in Brünnich's guillemots *Uria lomvia*. Briefly, I used the absolute densities of water, protein, lipid and ash (DeVries and Eastman, 1978; Lovvorn and Jones, 1991; Lovvorn et al., 1999) in conjunction with the mass ratios of these components in a common guillemot (Furness et al., 1994), to find a composite estimate of the volume of the body tissues.

I summed the volume of the body tissues with the plumage and respiratory air volumes to calculate total body volume (L), and I divided this sum by the approximate mass of the bird (in kg) to find the bird's above-water density (kg L^{-1}). During a dive, air volumes decrease by a factor of $10/(n+10)$ where n is depth in meters. Thus, the absolute density of a bird was calculated by reducing the air volumes as a function of depth and dividing this depth-dependent body volume estimate by the bird's body mass. Per kilogram buoyancy force was then calculated as $(\rho_w-\rho_d)9.806/\rho_d$, where ρ_w is the density of water (1 kg l^{-1}), ρ_d is depth-dependent density, and 9.806 is the force of gravity (in N kg^{-1}). Multiplying this result by the bird's approximate mass gave the absolute buoyancy force adjusted for depth.

Because capturing the SeaWorld birds would entail a stressful disturbance, I could not weigh the birds observed in this study. Thus for the purposes of calculating buoyancy, I assumed a mass of 1 kg for common murres and 0.8 kg for tufted puffins. I examined the potential for violation of this assumption to reduce the accuracy of my results by calculating dive parameters for 12 haphazardly selected common murre dives, once with the mass of the bird changed to 1.15 kg (15% increase) and again with the bird's mass set at 0.85 kg. I then compared work-per-flap estimates from these calculations using the increased and decreased masses with estimates based on the original masses to determine how sensitive my results would be to changing the mass parameter.

To move themselves forward diving birds must generate a

propulsion force equal to the sum of the drag on the bird's body and the upward force of buoyancy. Given that the pull of buoyancy was always directly upward and that the drag vector was always in the opposite direction of the bird's displacement, it was possible to calculate instantaneous resistance force that must be equaled by wing propulsion by summing the buoyancy and drag vectors. Assuming that the rate of displacement was constant over the given time interval (this assumption is addressed in the Discussion), I could then calculate the work (force×displacement) done during a flap cycle, and generate an estimate of cost of transport (COT), a dimensionless measure of the amount of work involved in moving a given mass a given distance (work×mass^{-1}×displacement^{-1}). I could also examine average power over a flap cycle (work×time^{-1}). The beginning of a given flap cycle as well as the end of the previous one was delineated by the wing tips reaching their lowest position relative to the bird's body. Only dives with constant flapping were analyzed in this study, and dives or parts of dives with noticeable glide phases were excluded from the data set.

I generated dive parameters from the video footage using two different general techniques. Initially I took position coordinates of the bird's head (the most reliable morphological landmark in my low-resolution video) at each frame throughout a dive. After generating three-dimensional coordinates, I applied a mild smoothing function (a moving average that spanned 5 coordinates for each axis) to these data to minimize the effects of small mouse-clicking errors when using CamMotion. I used these smoothed coordinates to calculate the amount of displacement that occurred between each video frame as well as the angle of descent and absolute depth. I then revisited the video footage and used CamMotion to record the time at which each flap cycle was completed (i.e. when the wing tip was at its lowest position relative to the bird's body). The total displacement that occurred over each flap cycle was found by summing the displacement values from each frame. Dividing the displacement over each interval by 1/30 of a second yielded a speed estimate, which could be used to calculate drag. From these nearly instantaneous drag estimates followed estimates for work and power associated with each 1/30 s time interval, which I summed over each flap cycle to generate per-flap estimates of these dive parameters.

Because this technique generally required the digitization of over 100 coordinates for each dive, I devised a less labor-intensive means of generating estimates of dive speed and depth, which I refer to as the shortcut technique. The shortcut technique involved recording the position of a bird's head only at the end of each flap cycle, rather than recording coordinates for each frame. Thus, the time marks for each flap and the coordinate data were recorded simultaneously, and there were generally less than 15 data points for each dive – one for each flap. Unlike the first technique, values for displacement, work, power, etc. were not derived by summing incremental values over a dive, but were simply calculated based on the change in a bird's position at the end of each flap cycle.

Molt monitoring

The SeaWorld husbandry staff at the Penguin Encounter generally try to avoid all unnecessary disturbances to their birds. Thus, it was not possible to capture birds in order to monitor molt in a quantitative way (e.g. by measuring the growth of new feathers). However, because feather loss was rapid and quite obvious in the birds I studied and because the birds were easily observed at close range through the viewing window, I was able to assess qualitatively the extent of wing molt in individual birds using binoculars or a video camera. These observations involved closely watching individual birds when they seemed prone to frequent stretching and preening of the wings and noting the extent to which the primaries and secondaries had been lost or replaced. From these observations I identified four somewhat distinct stages of flight-feather molt as follows: stage 1, all primaries missing and all or most secondaries remaining; stage 2, all primaries and secondaries missing; stage 3, new primaries emerged just beyond primary coverts; stage 4, primaries visible well beyond primary coverts and secondaries visible beyond secondary coverts (Fig. 2).

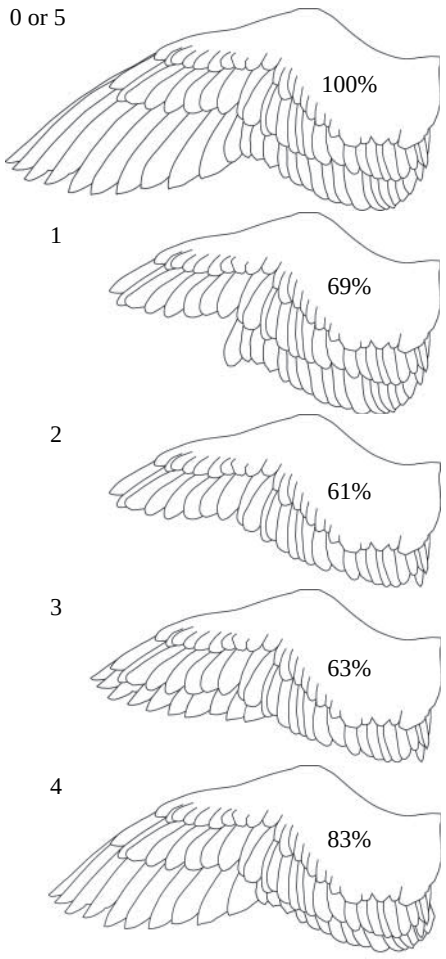

Fig. 2. Illustrations of wing-molt stages traced from photographs of a tufted puffin wing. All wings are drawn to the same scale. Approximations of the percentage of intact wing area with the wing loosely extended are listed for each molt stage.

I designated pre- and post-wing-molt plumages as stage 0 and stage 5, respectively. Fig. 2 shows approximate changes in wing surface area associated with each molt stage, based on photographs of a dead tufted puffin. Intermediate stages (e.g. roughly half of the primaries missing) were noted as such, and dives performed during these intermediate molt stages were not used for biomechanical analyses.

I calculated the approximate duration of each molt stage in both species by averaging the molt stage durations for which I had sufficient observations to distinguish an approximate beginning and end. The durations of intermediate molt stages were divided equally between the preceding and following stages for the purpose of calculating the average duration of each molt stage.

Statistical analysis of dive parameters

Because individual birds were identified as they dived, I tested for the effects of wing molt on the dive parameters using repeated-measures analysis of variance. This analysis used a within-subjects approach to test whether measurements made during any of the four stages of molt deviated significantly from baseline measurements obtained when a bird's wings were intact. Due to limited time for video footage collection, molt stage 0 was represented by only two birds among the common guillemots and molt stage 5 was not represented among the tufted puffins. Thus, I combined molt stages 0 and 5 to produce baseline values representative of the fully plumaged wing for comparison with different molt stages. I used Tukey–Kramer adjustments for multiple comparisons to determine statistical differences among the molt stages based on the magnitude of the deviations from baseline measurements.

The amount of usable dive footage obtained varied greatly among individual birds for different molt stages. Of the 40 common guillemots in the Penguin Encounter, there was sufficient footage for only 15 birds. Similarly the data for tufted puffins came from a total of 12 birds. For many of the birds that contributed to the analyzed data set, there was not sufficient dive footage to provide sets of dive parameters for some stages of molt. Molt stage 4 for tufted puffins was especially poorly represented by only three birds. Although I did not define a minimum acceptable quantity of data (i.e. a minimum number of flaps or dives) for inclusion of a bird mean in the analyzed data set, I endeavored to ensure that each bird's

Table 1. *Sample sizes for individual birds at different molt stages*

Species	SeaWorld ID code	Stage 0 or 5	Stage 1	Stage 2	Stage 3	Stage 4
Guillemot	1	(9) 54	–	(3) 23	(4) 27	(4) 39
Guillemot	2	(4) 19	–	(3) 20	(4) 26	(3) 19
Guillemot	7	(4) 35	–	(3) 28	(4) 36	(4) 32
Guillemot	15	(5) 41	(3) 20	(4) 45	(5) 41	(3) 23
Guillemot	17	(2) 12	(4) 22	(3) 19	(4) 23	(3) 27
Guillemot	18	(3) 27	(3) 26	(4) 30	(4) 39	–
Guillemot	52	(4) 29	(3) 25	(3) 27	(4) 35	(3) 21
Guillemot	55	(4) 24	(3) 24	(3) 37	(4) 29	(4) 32
Guillemot	179	(4) 35	(4) 21	(4) 21	(4) 44	(4) 37
Guillemot	188	(3) 21	(2) 22	(4) 30	(4) 38	(3) 26
Guillemot	190	(4) 29	(4) 27	(3) 18	(5) 34	–
Guillemot	196	(4) 24	(1) 10	(3) 25	(4) 28	(4) 31
Guillemot	197	(3) 21	–	(7) 67	(4) 39	(1) 11
Guillemot	199	(4) 33	(4) 33	(4) 30	(4) 25	(4) 40
Guillemot	200	(4) 28	(4) 29	(2) 20	(4) 35	–
Puffin	2	(5) 40	(4) 33	(4) 34	(3) 25	–
Puffin	17	(4) 21	–	(2) 14	(4) 22	–
Puffin	21	(3) 14	(2) 12	(2) 11	(4) 17	–
Puffin	127	(3) 21	(1) 13	(4) 28	(1) 7	–
Puffin	136	(1) 6	(2) 23	–	(4) 31	–
Puffin	155	(3) 19	–	–	(1) 6	(3) 26
Puffin	159	(3) 29	(2) 25	(4) 43	(4) 36	(2) 21
Puffin	162	(2) 14	(4) 22	(4) 28	(5) 35	(4) 29
Puffin	163	(3) 15	(3) 20	–	–	–
Puffin	171	(3) 18	(4) 29	(4) 23	(3) 14	–
Puffin	172	(4) 28	(4) 30	–	–	–
Puffin	186	(1) 5	(1) 7	(1) 5	(1) 6	–
Guillemot TOTAL		(61) 432	(35) 259	(53) 440	(62) 499	(40) 338
Puffin TOTAL		(35) 230	(27) 214	(25) 186	(30) 199	(9) 76

In all molt stage columns, numbers in parentheses indicate the number of dives, and numbers outside parentheses are the number of flaps.

mean for a given molt stage was derived from 20 or more flaps when sufficient footage was available. Table 1 lists the quantities of data that contributed to the individual bird means used for statistical testing.

Results

Validation of measurement system

Examination of the effects of increasing and decreasing assumed bird mass in 12 common murre dives indicated that variation in bird mass had little influence on the parameters used in the statistical analysis. Work per flap from the 12 dives averaged 1.50±0.24 J (mean ± S.D.) when assumed bird mass was 1 kg and changed insignificantly to 1.51±0.24 J and 1.49±0.24 J when bird mass was decreased and increased by 15%, respectively (ANOVA: $F_{2,33}$=0.027, P=0.97). Because this study employed primarily within-subjects analyses, I also examined the 66 possible pairwise differences among the 12 dives used for this sensitivity analysis. Averages of pairwise differences changed less than 0.01 J in association with a 15% increase and decrease in assumed bird mass. With regard to individual parings, among the 66 comparisons, increasing assumed mass by 15% caused qualitative (i.e. positive to negative) changes in the differences of three pairings, each of which had a difference of nearly zero. Decreasing the mass caused only one qualitative change in the 66 comparisons. Thus, I concluded that my results would be robust to any realistic amount of variation about the assumed bird masses, especially given the within-subjects approach to the data analysis.

Twenty-one measurements of a 0.56 m length of pipe positioned haphazardly in various positions throughout the visible portion of the diving pool averaged 0.556±0.017 m (mean ± S.D., range 0.534–0.595 m). There was no apparent pattern to errors in these measurements associated with the position of the pipe with respect to any of the three axes. Thus, coordinate data throughout the visible portion of the diving pool were equally valid.

Comparisons of the two techniques used to generate dive parameters (i.e. using coordinates from each frame of video *versus* using only the frames that depict the end of a flap cycle) indicated that they give equivalent qualitative results (Fig. 3). However, the shortcut technique yielded slightly lower values for some parameters, primarily because the displacement during any flap cycle was minimized (i.e. straightened). Nevertheless, the labor-saving advantages of the shortcut technique outweigh this minor inaccuracy, which is unlikely to have an appreciable effect of the results. Thus, with the exception of Fig. 3, all data presented here were generated by the shortcut technique.

Changes in dive parameters associated with wing molt

Wing molt was associated with clear decreases in flap duration for both common guillemots ($F_{4,62}$=8.24, P<0.001) and tufted puffins ($F_{4,38}$=5.85, P<0.001) for all stages of molt except stage 4 (Fig. 4A). For both species, the relative decreases

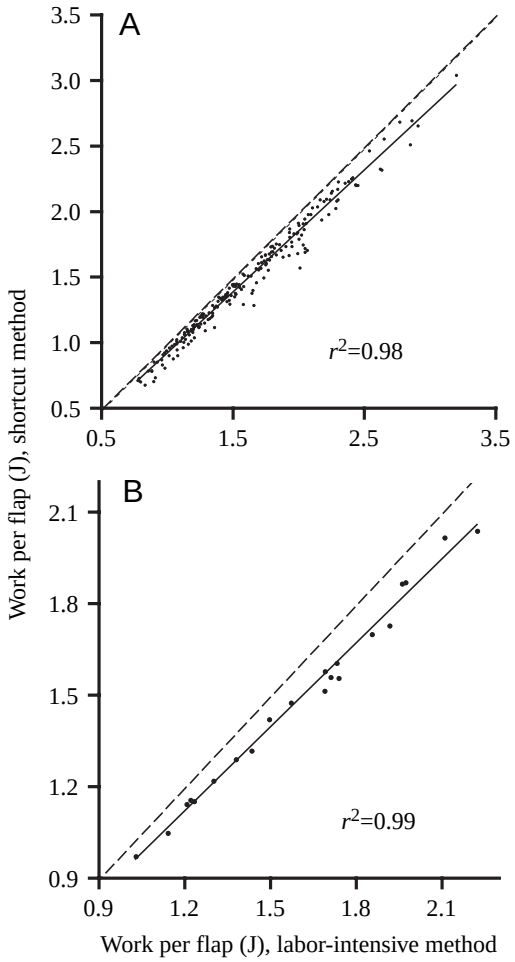

Fig. 3. Comparisons of labor-intensive and shortcut methods of estimating dive parameters. (A) Estimates of work per flap for 210 flaps derived independently by both techniques. (B) Estimates of work per flap from 21 dives with flaps from the same dive averaged. The number of flaps per dive ranged from 7 to 12 and averaged 10. All data points lie below the line of equality (broken line), indicating that slightly lower values were generated by the shortcut technique.

in flap duration associated with molt stages 1, 2 and 3 did not differ significantly from one another according to Tukey–Kramer multiple comparisons tests (α=0.05). Some stages of wing molt also appeared to decrease the average displacement achieved during a flap in both species (guillemots $F_{4,62}$=6.36, P<0.001; puffins: $F_{4,38}$=4.80, P=0.003; Fig. 4B). Despite these changes in flap duration and displacement during wing molt, average speed (calculated as displacement/duration) did not change significantly in association with molt stage (guillemots $F_{4,62}$=1.23, P=0.31; puffins: $F_{4,38}$=1.00, P=0.42; Fig. 4C). Because molt shortened the distance covered over each flap cycle, one would expect a corresponding decrease in work per flap. However, work per flap did not decrease significantly in common guillemots when comparing means from all molt stages ($F_{4,62}$=1.73, P=0.15; Fig. 4D), perhaps because of small insignificant increases in speed associated with some molt stages, and there was only a near-significant decrease

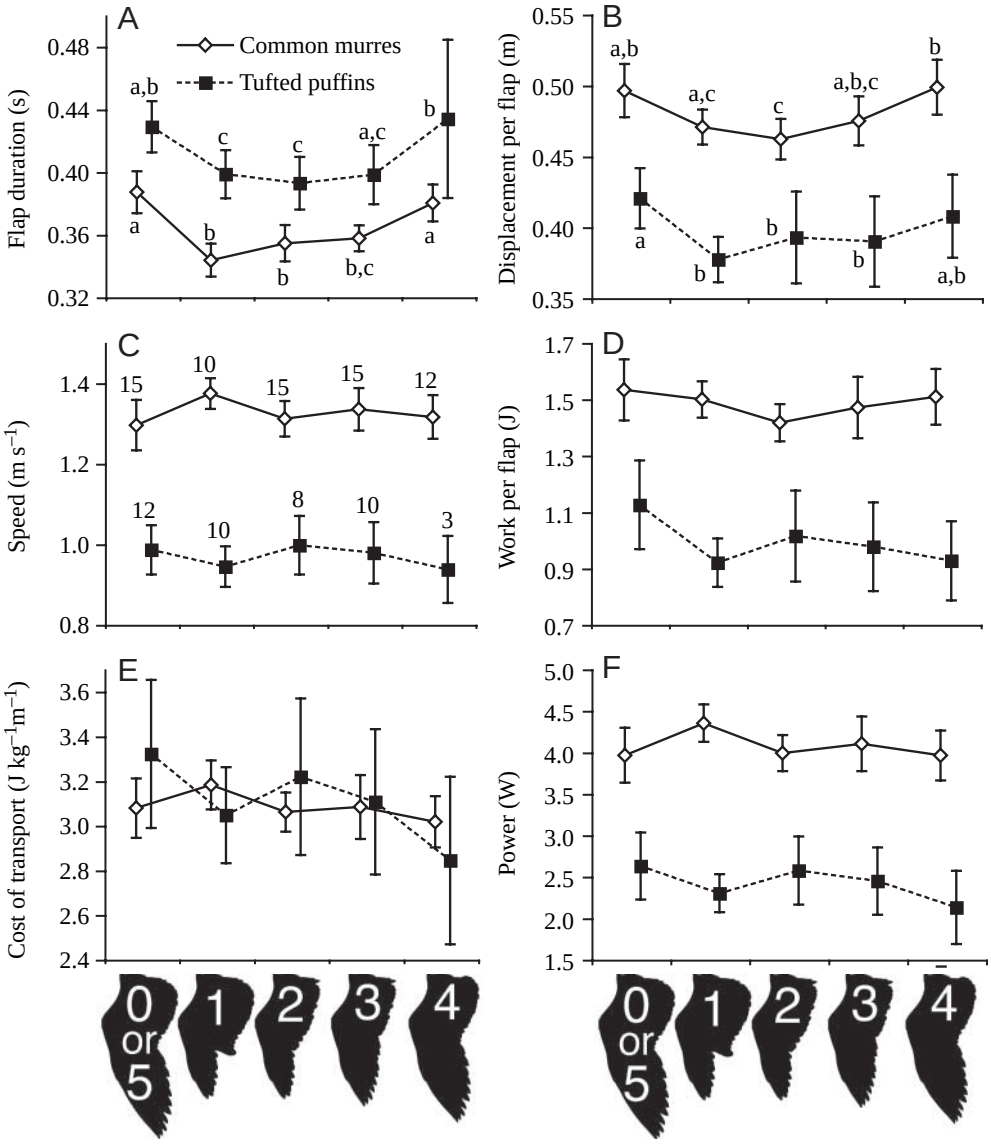

Fig. 4. Changes in dive parameters associated with each molt stage (illustrated along the *x* axis). The first (leftmost) point in each series is the overall mean from all birds for molt stages 0 and/or 5. The following points represent average deviations from that baseline mean. See text for details. Sample sizes (number of birds) are shown in C, with further details in Table 1. Error bars represent 95% confidence intervals. Lowercase letters indicate the results from Tukey–Kramer multiple comparisons tests; means that have a lowercase letter in common are not significantly different (α=0.05). If no letters are present then none of the means differ significantly.

in work per flap in tufted puffins ($F_{4,38}$=2.43, P=0.064; Fig. 4D). Notably, 14 of 15 guillemots in molt stage 2 showed a decrease in work per flap when compared to baseline values, and this general decrease is significantly different from zero in a simple two-tailed *t*-test that ignores multiple comparisons (t_{14}=–3.62, P=0.003). Dive angle, which was also a potentially important determinant of work, did not change significantly in response to molt (guillemots $F_{4,62}$=0.66, P=0.62; puffins: $F_{4,38}$=0.42, P=0.80; not shown). COT did not change significantly as a result of wing molt (guillemots $F_{4,62}$=0.99, P=0.42; puffins: $F_{4,38}$=0.1.00, P=0.42), and was roughly equal for both guillemots and puffins (Fig. 4E). Similarly, power averaged over the flap interval was not strongly affected by wing molt (guillemots $F_{4,62}$=1.32, P=0.27; puffins: $F_{4,38}$=0.1.07, P=0.38; Fig. 4F)

Molt observations

Average durations for each molt stage of each species are shown in Fig. 5. Interestingly, the onset of primary and secondary molt were offset in both species such that secondary molt began roughly 12 days after primary molt. Because many of the primaries are considerably longer than the secondaries, the primaries required more time to grow, so growth of both primaries and secondaries culminated at roughly the same time.

Discussion

Adaptive significance of intense wing molt and high wing loading

The primary effect of molt on diving evident in this study appears to be more frequent flapping both in terms of time and distance. My findings concur with those of Swennen and Duiven (1991) in that there was no significant change in diving speed associated with wing molt. However, I question their conclusion that flight-feather molt has no effect on diving

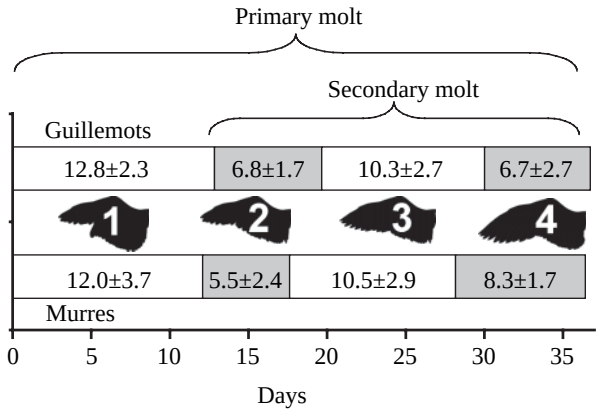

Fig. 5. Wing-molt chronology for common guillemots and tufted puffins. The durations of each molt stage are listed (mean ± S.D.). Brackets illustrate the approximate periods of primary and secondary molt. Respective sample sizes for molt stages 1–4 were 10, 17, 23 and 22 in common guillemots and 24, 31, 19 and 5 in tufted puffins.

ability as this study shows consistent decreases in the amount of work done during a flap. Furthermore, the increased flap rate may indicate that more muscular work is required to maintain a constant speed.

Because wing molt had no positive effects on any of the diving parameters, it is unlikely that the evolution of intense molt in alcids was favored by diving biomechanics as some have speculated (Gaston and Jones, 1998; Thompson et al., 1998). The more generally accepted explanation for intense wing molt in alcids and other species with high wing loading (e.g. waterfowl) postulates that almost any reduction in wing area, even that resulting from a relatively slow sequential wing molt, would cause wing-loading to approach the theoretical maximum for aerial flight, approximately 2.5 g cm^{-2} (Meunier, 1951; Storer, 1960, 1971; Warham, 1977; Pennycuick, 1987; Livezey, 1988). In other words, the loss of one or two feathers, as would occur with a gradual molt, may render a bird with especially high wing loading flightless, or nearly so. Thus, intense molt probably evolved as a means of shortening the molting period and of avoiding some of the potential costs associated with a prolonged molt-induced disruption of flight ability.

Although there often was not sufficient resolution in the data to distinguish the relative degrees to which different stages of molt diminished diving efficiency, it is notable that flap duration was at its lowest during molt stage 2 in both study species, and measurements associated with molt stage 4 indicated less severe affects on most diving parameters. Thus, the detrimental effects of wing molt are to some degree proportional to the extent of wing-area reduction, and the fact that secondary molt began roughly 12 days after the initiation of primary molt could be viewed as an adaptation to reduce the duration of molt stage 2, wherein both primaries and secondaries are missing (or have yet to emerge beyond the coverts). Delaying the onset of secondary molt allows partial regrowth of the primaries before the secondaries are lost, preserving wing surface area to some degree and shortening the period of time during which neither primaries nor secondaries extend beyond their respective coverts. Feathers of all bird species grow at roughly the same rate (3–5 mm day^{-1}), regardless of the size of the fully grown feather (Prevost, 1983; Langston and Rohwer, 1996; Prum and Williamson, 2001; Dawson, 2003). Therefore, because most of the primaries are considerably longer than the secondaries, the primaries take longer to completely regrow. Consequently, delaying secondary molt results in both primary and secondary growth culminating at approximately the same time, so delaying the onset of secondary molt does not appear to lengthen the molting period (Fig. 5).

The fact that reduced wing area failed to improve diving efficiency suggests that the evolution of small wings and high wing loading may not be an adaptation for improved diving ability as previously thought (Storer, 1960; Stresemann and Stresemann, 1966; Ashmole, 1971; Pennycuick, 1987). Lovvorn and Jones (1994) argue convincingly that the small, pointed wings of alcids and many other open-water birds are an adaptation associated with maximizing high-speed, long-distance flight efficiency at the expense of maneuverability. They point out that an open-water habitat relaxes selective pressure for highly maneuverable flight at low speeds, as is needed to land on perches and to be able to escape predators by rapid, vertical take-off. As a consequence, many aquatic birds have adopted a style of flight that uses small, rapidly beating wings to generate high flight speed, which may be useful for rapid movements between specialized habitats. The extremely long-winged seabirds such as shearwaters and albatrosses (Procellariiformes) have presumably adopted an alternative flight strategy wherein they use their long wings for energetically efficient dynamic soaring, sacrificing both high flight speed and some degree of maneuverability. Lovvorn and Jones (1994) also note that many birds that do not practice wing-propelled diving, such as waterfowl (anseriformes), grebes (Podicepidiformes), and loons (Gaviformes), have adopted similarly high wing loading and rapid-stroke flying dynamics in association with an open water habitat. Furthermore, there are several long-winged seabirds that demonstrate diving behavior comparable to that of alcids. For instance, wedge-tailed shearwaters *Puffinus pacificus*, Audubon's shearwaters *Puffinus lherminieri*, short-tailed shearwaters *Puffinus tenuirostris*, black-vented shearwaters *Puffinus opisthomelas*, and sooty shearwaters *Puffinus griseus* all dive to depths exceeding 20 m, with some individuals reaching 70 m depth (Morgan, 1982; Weimerskirch and Sagar, 1996; Keitt et al., 2000; Burger, 2001), and there is evidence of wing-propelled diving among boobies and gannets as well (Adams and Walter, 1993; Le Corre, 1997). Thus, it would appear that the evolution of small wings is less relevant to wing-propelled diving than many have suggested (e.g. Storer, 1960; Stresemann and Stresemann, 1966; Ashmole, 1971; Pennycuick, 1987).

Limitations of study system

A critical assumption to the quasi-steady modeling approach

that allowed for my calculations of drag is that flow over the surface of the bird is fully developed at each different speed over each time interval. Because fully developed flow does not occur instantaneously, this assumption is technically incorrect. Direct studies of unsteady flow are thus far limited to rigid structures under carefully controlled conditions (Dickinson, 1996), and the complexity of unsteady (as opposed to quasi-steady) flow theory makes it unsuitable for most applied problems involving flapping propulsors. Thus, the quasi-steady approach is the best available method for investigating the effects of wing molt on diving.

This study differs from the standard approach to quantitative biomechanical studies in that it forgoes any attempt to generate highly accurate measurements from a small number of samples in favor of generating a large data set with less accurate measurements. Due to limitations in the study system, there are several potential sources of measurement error in this study that should be addressed. First of all, it is important to regard the dive parameters reported in this study more as indices than absolute measurements. One reason for this distinction is that the relationship between speed and drag is not linear. In calculating the work done over an entire flap I used the average speed to derive the drag force, which amounts to assuming a uniform speed throughout a flap cycle. However, it has been demonstrated that instantaneous velocity varies considerably during a flap in association with both upstroke and downstroke components (Lovvorn et al., 1999, 2001; Lovvorn, 2001; Lovvorn and Liggins, 2002). Because drag increases exponentially with speed, fluctuations in speed could give rise to disproportionate fluctuations in drag, such that only instantaneous speed and drag measurements can provide extremely accurate estimates of work and power by integrating over a time interval.

Secondly, the shortcut method used to generate coordinate data may have resulted in underestimated speed, work, and power (see Fig. 4). Average non-molting dive speeds in this study were 1.32 m s^{-1} and 0.99 m s^{-1} for common guillemots and tufted puffins respectively. In other studies of alcids, estimates of dive speed are generally higher. Swennen and Duiven (1991) estimated the mean level swimming speed of common guillemots at 2.18 m s^{-1}, and according to Croll et al. (1992) free-swimming Brünnich's guillemots averaged 1.52 m s^{-1}. Similarly, Atlantic puffins *Fraturcula arctica* swimming in a confined dive tank demonstrated speeds ranging from 1.02 to 2.14 m s^{-1} (Johansson and Wetterholm Aldrin, 2002).

Finally, as mentioned earlier, actual masses of the birds (a component of buoyancy calculations) were unknown because frequent weighing would violate SeaWorld's husbandry policy. However, I suspect that the minor inaccuracies in some dive parameters associated with the lack of mass data are rendered negligible in terms of testing the effects of molt because of the within-subjects experimental design, which negates variation among birds.

Despite these potential problems, my approach seems suitable for testing for effects of molt on diving ability, at least in a qualitative sense. Discrepancies between dive speeds observed in this study and others may be due to factors other than measurement techniques, such as the nature and intensity of a bird's motivation to dive. There was rarely any clear motivation for any of the dives examined in this study, whereas the birds in other studies were diving for food (Swennen and Duiven, 1991; Croll et al., 1992) or in response to a startle stimulus (Johansson and Wetterholm Aldrin, 2002).

Extrapolation to wild birds

Perhaps of greater concern than measurement error is the possibility that wing molt as I observed it in SeaWorld's captive alcids may differ from what occurs in wild birds. Molt is generally triggered by changes in day length, and SeaWorld's birds were exposed to natural daylight *via* several large skylights in their aviary. SeaWorld's birds included individuals captured as wild adults (mostly from high-latitude populations) as well as captive-born birds. Because of the skylights in the birds' habitat, it was impossible to shorten day lengths during the winter. Thus, molting schedules in these birds evolved under a day-length regime with greater seasonal variability than occurs in SeaWorld's location in southern California.

Nevertheless, my observations of molt at SeaWorld do not appear to differ substantially from the reports of molt in wild alcids. The most comprehensive treatment of molt in common guillemots is that of Thompson et al. (1998), who determined the pattern and timing of molt from wild birds killed by gill net fisheries. They found that the duration of a molt cycle was highly variable, ranging from 24 to 81 days with large differences between the 2 years of their study. The findings of this study and other estimates of wing-molt duration in common terns generally fall within this range (Glutz von Blotzheim and Bauer, 1982; Ginn and Melville, 1983; Harris and Wanless, 1988). Furthermore, the delaying of secondary molt with respect to primary molt was documented by Thompson et al. (1998), who observed secondary molt beginning and finishing when the primaries were 27% and 99% grown, respectively. Birkhead and Taylor (1977) offer a similar finding, with secondary molt beginning and finishing when the primaries were 38% and 99% grown, respectively. Thus, my observations of molt in SeaWorld's common guillemots correspond with what occurs in the wild, and I think that my conclusions regarding the evolutionary significance of offsetting primary and secondary molt are relevant to wild common guillemots.

It is less clear whether captive tufted puffins accurately reflect wing molt in wild birds. My observations generally agree in terms of molt duration and offsetting primary and secondary molt with a separate study of captive tufted puffins undergoing their first wing molt (Thompson and Kitaysky, 2004). Unfortunately, detailed molt data from wild tufted puffins is lacking, but there is documentation of molt in Atlantic puffins that states that these birds do not lose their secondaries until their primaries have emerged from their sheaths (Harris and Yule, 1977), indicating a delay in the

onset of secondary molt as observed in SeaWorld's tufted puffins.

Suggestions for future studies

Although this study reveals increases in flap rates and relatively constant or slightly reduced work per flap for birds in molt, the effects of the substantial loss of wing area caused by intense molt were surprisingly small with regard to cost of transport and power output. The absence of strong effects on these and other parameters suggests that alcids may alter their wing-stroke biomechanics to compensate for their missing wing feathers. Thus, in addition to studying the gross effects of wing molt on wing-propelled diving, it would also be of interest to investigate whether alcids make adjustments in diving parameters such as stroke volume (i.e. the volume that contains the plane of the wing throughout a stroke), angles of attack at given points of the upstroke and downstroke, and rotational velocity of the wings in response to wing molt. Molting alcids may also extend their wings to a greater extent when diving to effectively increase their wing surface area. Techniques outlined by Johansson (2003) and Johansson et al. (2002) would allow for a good evaluation of these variables with regard to the potential effects of wing molt.

It would also be of interest to examine how molt affects diving ability in smaller alcids that undergo rapid wing molt. This excludes the *Aethia* and *Ptychoramphus* auklets, which molt their wing feathers gradually (Thompson and Kitaysky, 2004), but includes species such as dovekies *Alle alle* and marbled murrelets *Brachyramphus marmoratus*, which are roughly half the body length and a third the mass of common murres. Diving petrels, which are of similar size to the smallest alcids, might also be considered for further study of wing-molt biomechanics as some species appear to have a rapid wing molt similar to that of alcids (Watson, 1968). Because these smaller birds carry much less inertial mass through the water and have somewhat lower wing loading than many larger alcids, rapid wing molt may have different effects on diving efficiency.

A molting alcid must contend with the energetic demands of feather growth in addition to the lack of mobility associated with flightlessness. Thus, an improved understanding of the effects of intense wing molt on diving and foraging could provide key insights into how these birds survive this potentially stressful period. As researchers pursue the development of biomechanical models for describing wing-propelled diving, I suggest that they consider the effects of wing molt and generate testable hypotheses regarding how this phenomenon affects birds in the field.

Seaworld San Diego has my eternal gratitude for accommodating this project. Specifically, I thank Janet Edwards and Stephanie Costellow for logistical aid, Steve Norby for helping with the camera array, and the Penguin Encounter husbandry staff for sharing their knowledge and workspace. Funding for this project was provided by Dayton Wilkie Natural History Fund, Sigma Xi Grants in Aid of Research, and a National Science Foundation Doctoral Dissertation Fellowship.

References

Adams, N. J. and Walter, C. B. (1993). Maximum diving depths of Cape Gannets. *Condor* **95**, 734-736.

Ashmole, N. P. (1971). Sea bird ecology and the marine environment. In *Avian Biology*, vol. I (ed. D. S. Farner and J. R. King), pp. 223-286. New York: Academic Press.

Birkhead, T. R. and Taylor, A. M. (1977). Moult of the Guillemot *Uria aalge*. *Ibis* **1199**, 80-85.

Bridge, E. S. (2003). Effects of simulated primary moult on pigeon flight. *Ornis Fennica* **80**, 121-129.

Burger, A. E. (2001). Diving depths of shearwaters. *Auk* **118**, 755-759.

Chai, P., Altshuler, D. L., Stephens, D. B. and Dillon, M. E. (1999). Maximal horizontal flight performance of hummingbirds: effects of body mass and molt. *Physiol. Biochem. Zool.* **72**, 145-155.

Croll, D. A., Gaston, A. J., Burger, A. E. and Konnoff, D. (1992). Foraging behavior and physiological adaptation for diving in Thick-Billed Murres. *Ecology* **73**, 344-356.

Dawson, A. (2003). A detailed analysis of primary feather moult in the Common Starling *Sturnus vulgaris* – new feather mass increases at a constant rate. *Ibis* **145(online)**, E69-E76.

DeVries, A. L. and Eastman, J. T. (1978). Lipid sacs as a buoyancy adaptation in an Antarctic fish. *Nature* **271**, 352-353.

Dickinson, M. H. (1996). Unsteady mechanisms of force generation in aquatic and aerial locomotion. *Amer. Zool.* **36**, 537-554.

Ewins, P. J. (1993). Pigeon Guillemot. In *Birds of North America*, no. 49 (ed. F. Gill), pp. 1-24. Philadelphia, PA: Academy of Natural Sciences of Philadelphia and the American Ornithologists' Union.

Furness, R. W., Thompson, D. R. and Harrison, N. (1994). Biometrics and seasonal changes in body composition of Common Guillemots *Uria aalge* from north-west Scotland. *Seabird* **16**, 22-29.

Gaston, A. J. and Jones, I. L. (1998). *The Auks: Alcidae*. Oxford: Oxford University Press.

Ginn, H. B. and Melville, D. S. (1983). *Moult In Birds*. Tring, UK: British Trust for Ornithology.

Glutz von Blotzheim, U. N. and Bauer, K. M. (1982). *Handbuch der Vögel Mitteleuropas*. Weisbaden, Germany: Akademsche Verlagsgesellschaft.

Harris, M. P. and Wanless, S. (1988). Measurements and seasonal changes in weight of Guillemots *Uria aalge* at a breeding colony. *Ring. Migr.* **9**, 32-36.

Harris, M. P. and Yule, R. F. (1977). The moult of the Puffin *Fratercula arctica*. *Ibis* **119**, 535-541.

Hedenström, A. and Sunada, S. (1998). On the aerodynamics of moult gaps in birds. *J. Exp. Biol.* **202**, 67-76.

Hedenström, A. and Sunada, S. (1999). On the aerodynamics of moult gaps in birds. *J. Exp. Biol.* **202**, 67-76.

Johansson, L. C. (2003). Indirect estimates of wing-propulsion forces in horizontally diving Atlantic puffins (*Fratercula arctica* L.). *Can. J. Zool.* **81**, 816-822.

Johansson, L. C. and Wetterholm Aldrin, B. S. (2002). Kinematics of diving Atlantic puffins (*Fratercula arctica* L.): evidence for an active upstroke. *J. Exp. Biol.* **205**, 371-378.

Keitt, B. S., Croll, D. A. and Tershy, B. R. (2000). Dive depth and diet of the Black-vented Shearwater (*Puffinus opisthomelas*). *Auk* **117**, 507-510.

Klasing, K. C. (1998). *Comparative Avian Nutrition.* New York: CAB International.

Kovacs, C. E. and Meyers, R. A. (2000). Anatomy and histochemistry of flight muscles in a wing propelled diving bird, the Atlantic Puffin, *Fratercula arctica*. *J. Morphol.* **244**, 109-125.

Langston, N. E. and Rohwer, S. (1996). Molt-breeding tradeoffs in albatrosses: life history implications for big birds. *Oikos* **76**, 498-510.

Lasiewski, R. C. and Calder, W. A. (1971). A preliminary allometric analysis of respiratory variables in resting birds. *Resp. Physiol.* **11**, 152-166.

Le Corre, M. (1997). Diving depths of two tropical pelicaniformes: the Red-Tailed Tropicbird and the Red-Footed Booby. *Condor* **99**, 1004-1007.

Livezey, B. C. (1988). Morphometrics of flightlessness in the alcidae. *Auk* **105**, 681-698.

Lovvorn, J. R. (2001). Upstroke thrust, drag effects, and stroke-glide cycles in wing-propelled swimming birds. *Amer. Zool.* **41**, 154-165.

Lovvorn, J. R., Croll, D. A. and Liggins, G. A. (1999). Mechanical *versus*

physiological determinants of swimming speeds in diving Brünnich's guillemots. *J. Exp. Biol.* **202**, 1741-1752.

Lovvorn, J. R. and Jones, D. R. (1991). Effects of body size, body fat, and change in pressure with depth on buoyancy and costs of diving in ducks (*Aythya* spp.). *Can. J. Zool.* **69**, 2879-2887.

Lovvorn, J. R. and Jones, D. R. (1994). Biomechanical conflicts between adaptations for diving and aerial flight in estuarine birds. *Estuaries* **17**, 62-75.

Lovvorn, J. R. and Liggins, G. A. (2002). Interactions of body shape, body size and stroke-acceleration patterns in costs of underwater swimming by birds. *Funct. Ecol.* **16**, 106-112.

Lovvorn, J. R., Liggins, G. A., Borstad, M. H., Calisal, S. M. and Mikkelsen, J. (2001). Hydrodynamic drag of diving birds: effects of body size, body shape and feathers at steady speeds. *J. Exp. Biol.* **204**, 1547-1557.

Meunier, K. (1951). Korrelation und Umkonstruktion in den Grössenbeziehungen zwischen Vogelflugel und Vogelkörper. *Biol. Generalis* **19**, 403-443.

Montevecchi, W. A. and Stenhouse, I. J. (2002). Dovekie (*Alle alle*). In *Birds of North America*, No. 701. Philadelphia, PA: The Birds of North America, Inc.

Morgan, W. L. (1982). Feeding methods of the Short-tailed Shearwater (*Puffinus tenuirostris*). *Emu* **82**, 226-227.

Murphy, M. E. (1996). Energetics and nutrition of molt. In *Avian Energetics and Nutritional Ecology* (ed. C. Carey), pp. 158-198. New York: Chapman and Hall.

Murphy, M. E. and King, J. R. (1991). Nutritional aspects of avian molt. *Acta XX Congr. Int. Ornithol.* **IV**, 2186-2193.

Pennycuick, C. J. (1987). Flight of auks (Alcidae) and other northern seabirds compared with southern procellariifformes: ornithodolite observations. *J. Exp. Biol.* **128**, 335-347.

Prevost, Y. (1983). The moult of the Osprey *Pandion haliaetus*. *Ardea* **71**, 199-209.

Prum, R. O. and Williamson, S. (2001). Theory of the growth and evolution of feather shape. *J. Exp. Zool.* **291**, 30-57.

Raikow, R. J., Bicanovsky, L. and Bledsoe, A. H. (1988). Forelimb joint mobility and the evolution of wing-propelled diving birds. *Auk* **105**, 446-451.

Storer, R. W. (1960). Evolution in the diving birds. *Acta XVIII Congr. Int. Ornithol.* **II**, 694-707.

Storer, R. W. (1971). Adaptive radiation in birds. In *Avian Biology*, vol. 1 (ed. D. S. Farner, J. R. King and K. C. Parkes), pp. 149-188. New York: Academic Press.

Stresemann, E. and Stresemann, V. (1966). Die Mauser der Vögel. *J. Ornithol.* **107**, 1-448.

Swaddle, J. P., Williams, E. V. and Rayner, J. M. V. (1999). The effect of simulated flight feather moult on escape take-off performance in starlings. *J. Avian Biol.* **30**, 351-358.

Swaddle, J. P. and Witter, M. S. (1997). The effects of molt on the flight performance, body mass, and behavior of European Starlings (*Sturnus vulgaris*): an experimental approach. *Can. J. Zool.* **75**, 1135-1146.

Swennen, D. and Duiven, P. (1991). Diving speed and food-size selection in the Common Guillemots, *Uria aalge*. *Neth. J. Sea Res.* **27**, 191-196.

Thompson, C. W. and Kitaysky, A. S. (2004). Polymorphic flight-feather molt sequence in Tufted Puffins (*Fratercula cirrhata*): a rare phenomenon in birds. *Auk* **121**, 35-45.

Thompson, C. W., Wilson, M. L., Melvin, E. F. and Pierce, D. J. (1998). An unusual sequence of flight-feather molt in Common Murres and its evolutionary implications. *Auk* **115**, 653-669.

Tucker, V. A. (1991). The effect of molting on the gliding performance of a Harris' Hawk (*Parabuteo unicinctus*). *Auk* **108**, 108-113.

Walsberg, G. E. (1983). Ecological energetics: what are the questions? In *Perspectives in Ornithology* (ed. A. H. Brush and G. A. Clark), pp. 135-158. Cambridge, UK: Cambridge University Press.

Warham, J. (1977). Wing loadings, wing shapes, and flight capabilities of Procellariiformes. *NZ J. Zool.* **4**, 73-83.

Watson, G. E. (1968). Synchronous wing and tail molt in diving petrels. *Condor* **70**, 182-183.

Weimerskirch, H. and Sagar, P. M. (1996). Diving depths of Sooty Shearwaters *Puffinus griseus*. *Ibis* **138**, 786-794.

Williams, E. V. and Swaddle, J. P. (2003). Moult, flight performance, and wingbeat frequency during take-off in European starlings. *J. Avian Biol.* **34**, 371-378.

Wilson, R. P., Hustler, K., Ryan, P. G., Burger, A. E. and Noldeke, E. C. (1992). Diving birds in cold water: do Archimedes and Boyle determine energetic costs? *Am. Nat.* **140**, 179-200.